Lithuanian Journal of Physics, Vol. **47**, No. 2, pp. 129–135 (2007)

THE $4p^6$-CORE EXCITED AUTOIONISING STATES IN STRONTIUM: CLASSIFICATION AND EXCITATION DYNAMICS

A. Borovik [a], V. Vakula [a], and A. Kupliauskienė [b]

[a] *Institute of Electron Physics, National Academy of Sciences of Ukraine, Universitetska 21, UA-88017 Uzhgorod, Ukraine*
E-mail: sasha@aborovik.uzhgorod.ua

[b] *Institute of Theoretical Physics and Astronomy of Vilnius University, A. Goštauto 12, LT-01108 Vilnius, Lithuania*
E-mail: akupl@itpa.lt

Received 24 April 2007; revised 3 May 2007

The ejected electron spectra corresponding to the electron decay of the $4p^5n_1l_1n_2l_2n_3l_3$ low-lying autoionising states in strontium atoms were measured in the impact energy range from the excitation threshold of states up to 200 eV. By using the results of single-configuration Hartree–Fock (HF) calculations, six ejected electron lines with the lowest excitation thresholds were attributed to the decay of the $(4p^54d5s^2)\,{}^3\mathrm{P}_{0,1,2}$ and ${}^3\mathrm{F}_{2,3,4}$ autoionising states. For the ${}^3\mathrm{P}_{1,2}$ and ${}^3\mathrm{F}_4$ states the excitation functions were obtained at an incident electron energy resolution of 0.15 eV. In all excitation functions the strong near-threshold structure was revealed for the first time. The origin of the structure was attributed to the decay of short-lived states from the $4p^55s^24d^2$ configuration of Sr^- ion. The cascade population of the ${}^3\mathrm{P}_{0,1,2}$ and ${}^3\mathrm{F}_{2,3,4}$ states was considered by using the HF energies and decay probabilities for the $4p^55s^25p$ levels.

Keywords: autoionisation, cascade transition, negative-ion state, resonance

PACS: 32.80.Dz, 34.80.Dp, 31.50.Df, 39.30.+W, 13.40.Hg

1. Introduction

The excitation of the $4p^6$ subshell in strontium atoms results in creation of the $4p^5n_1l_1n_2l_2n_3l_3$ atomic autoionising states. Due to the fast electron decay (lifetime τ $\sim$$10^{-15}$–$10^{-13}$ s) such states contribute essentially to the single and double ionisation cross-section [1, 2] as well as to the excitation cross-section of Sr^+ ions [3]. Another interesting feature of the $4p^5n_1l_1n_2l_2n_3l_3$ states is their high excitation efficiency at low impact energies [4, 5]. These observations along with the well-known high polarizability of alkali-earth atoms [6] point out an important role of resonance processes in the electron impact excitation of the $4p^6$ subshell in strontium.

The first experimental observation of the resonance features in electron impact excitation of the $4p^6$ subshell in strontium was reported by Aleksakhin et al. [7]. In excitation functions of two spectral lines at 58.4 and 62.4 nm attributed to the radiative decay of the $4p^5n_1l_1n_2l_2n_3l_3$ autoionising states, the authors revealed strong maxima located at approximately 5 eV above the excitation thresholds of lines. Unfortunately, the authors did not discuss the origin of the observed features. Similar resonance-like features were later observed also in the ejected electron excitation functions for some of the $4p^5n_1l_1n_2l_2n_3l_3$ low-lying autoionising states [8]. The sharp increase of the cross-section just above the excitation threshold of states was explained by the authors as an influence of the short-lived negative-ion resonances. Although these data were obtained at an improved energy resolution of 0.3 eV, no resonance structure was revealed in the measured excitation functions.

The theoretical calculations of the $4p^6$ subshell excitation in strontium were performed earlier only with the aim of a spectroscopic classification of lines in ejected electron and photoabsorption spectra [5, 9, 10]. These data revealed the strong configuration mixing effects even in excitation of the lowest configurations $4p^54d5s^2$ and $4p^55s4d^2$. For these reasons the spectroscopic classification of the $4p^5n_1l_1n_2l_2n_3l_3$ atomic autoionising levels was established to present day only for some of the dipole-allowed transitions from the ground state into the $4d$, $4d^2$, and $6s$ states [9, 10]. The lack of reliable high-resolution experimental data on the excitation thresholds and excitation cross-sections of autoionising levels restrains the further development of theoretical approaches.

ISSN 1648-8504

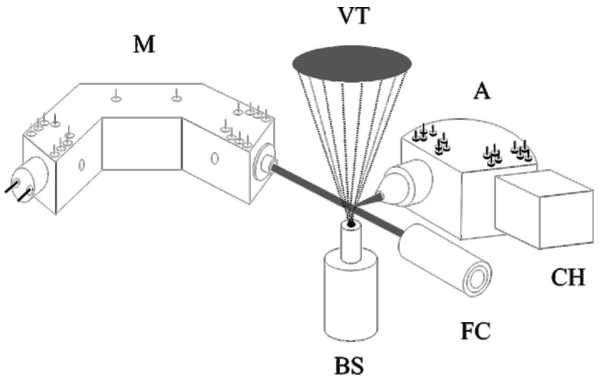

Fig. 1. The ejected electron spectrometer: M is monochromator of incident electron beam, A is analyzer of ejected and scattered electrons, BS is atomic beam source, CH is channel electron multiplier, FC is Faraday cup, VT is strontium vapour trap.

In the present work the ejected electron spectra corresponding to the $4p^5n_1l_1n_2l_2n_3l_3$ low-lying autoionising states were studied in the wide impact energy range from the excitation threshold of states up to 200 eV. By precise measurement with an energy resolution of 0.15 eV of the near-threshold impact energy region, the strong resonance structure was for the first time revealed in the excitation functions for ejected electron lines with the lowest excitation thresholds. The spectroscopic classification of these lines was established on the basis of single-configuration Hartree–Fock calculations. For analysing the excitation dynamics of classified autoionising states at threshold impact energies a comparison with *isoelectronic* configurations in yttrium atoms was used to identify the observed resonance structure. The calculated energies and decay rates for the $4p^55s^25p$ states were used to classify the cascade transitions.

2. Experimental details

The measurements were performed with an electron spectrometer consisting of a 127° electrostatic cylindrical analyzer of ejected electrons, a 127° electrostatic cylindrical monochromator of incident electron beam, and an atomic beam source. Figure 1 shows the general view of the spectrometer. The design of analyzer was similar to that described earlier in [11]. However, to avoid an influence of chemically active high-temperature strontium vapours on the performance of the analyzer, the electron optical lens system was made of molybdenum and non-magnetic stainless steel. For the minimization of the space charge formed by secondary electrons in the region of the central electron trajectory, the deflector plates were made of the tungsten mesh of 90% transparency. The input lens system was designed for providing about ±4° angular resolution of the analyzer. The flux of energy-selected electrons at the output of analyzer was detected by the channel electron multiplier VEU-6. The ejected electron spectra were detected at an observation angle of 75° and at an ejected electron energy resolution of 0.15 eV. The latter value was strongly limited by the extremely low intensity of ejected electron spectra measured at the threshold impact energies. The monochromator design was described earlier [12]. It produced an incident electron beam of $\leq$0.15 μA intensity in the energy range of 15–200 eV. The energy spread of the beam at energies below 50 eV did not exceed 0.15 eV, and this was controlled by measuring the elastic peak in the energy loss spectra of scattered electrons. A resistively heated oven similar to that described in [13] was used for producing the well-collimated strontium vapour beam with the density of about 10^{12} at cm^{-3} in the interaction region. The beam was formed by the 'hot' 0.4×3 mm^2 slit located at the output end of the transportation channel 40 mm long and 3 mm in diameter. The angular spread of the beam did not exceed 90°.

The measurement and data processing procedures both were described in detail earlier [14, 15]. Briefly, the ejected electron spectra corresponding to the decay of the $4p^5n_1l_1n_2l_2n_3l_3$ autoionising states were measured in series, step-by-step for different incident electron energy values over the range from the lowest excitation threshold of levels up to 200 eV. In the near-threshold energy region of 21–24 eV, the increment step of the incident energy was 50 meV. The spectra were automatically normalized to the intensity of the incident electron beam by a 'current-to-frequency' converter. All measured spectra were processed for subtracting the background intensity and for deriving the line intensities. Because the atomic autoionising states in strontium posses the multichannel decay mode [5, 8], the strongest lines reflecting the decay into the $(4p^65s)\,^2\mathrm{S}_{1/2}$ ground state of Sr II were used for obtaining the excitation functions of corresponding states. The statistical error, depending on the relationship between the line intensities and the nonlinear background function, did not exceed 15% for most of the data obtained at impact energies 0.1 eV above the excitation threshold of levels. Note that due to a limited energy resolution of the analyzer, the accuracy of data was additionally affected by overlap of the lines under study and the neighbouring lines. Therefore, the combined relative uncertainty, after ac-

counting also for fluctuations of the experimental conditions, varied from 20 to 35%. For the first two and the last points of all excitation functions this uncertainty reached the value of 50%. Furthermore, in the energy region 34–38 eV the accuracy was adversely affected by overlap of the ejected electron spectra with the associated $4p^5n_1l_1n_2l_2n_3l_3$ energy loss spectra. The data obtained in three independent experiments were compared and averaged over the energy positions and intensities of the lines. The incident electron and ejected electron energy scales were calibrated by using photoabsorption data [8] for the excitation threshold of the $(4p^55s^2)\,^2\mathrm{P}_{3/2}$ ionic state at 28.178 eV. The uncertainties of both energy scales were estimated as $\pm$100 meV and $\pm$50 meV, respectively.

3. Theoretical approach

In the case of the autoionising states, the correlation effects play an important role. But, for the lowest core-excited levels of Na [16] and K [17], a better agreement was noticed between experimental excitation energies and those of single-configuration Hatree–Fock rather than the large scale configuration interaction results. It happened due to the cancellation of correlation contributions in the initial and final states. Therefore, the theoretical values of the lowest energy levels in $4p^65s^2$, $4p^54d5s^2$, $4p^55s4d^2$, and $4p^55s^25p$ configurations, as well as wavelengths and probabilities for the $(4p^55s^25p)\,L_2S_2J_2 \rightarrow (4p^55s4d^2)\,L_1S_1J_1$ radiative transitions were calculated in single-configuration Hatree–Fock approximation by using the complex of computer programs [18]. The radial wave functions were obtained by solving the non-relativistic Hartree–Fock equations. The energies and state wave functions were found in the intermediate coupling approximation by diagonalizing the energy matrix of the non-relativistic Hamiltonian including the Breit–Pauli relativistic corrections of up to the second order in the fine structure constant α, i. e. α^2.

The calculated energies for the lowest states of the $4p^54d5s^2$ and $4p^55s4d^2$ configurations with respect to the ground state of strontium atom are presented in Table 1. The calculated oscillator strengths for electric dipole (E1) and magnetic quadrupole (M2) transitions and the values of energies of the present experiment are also included into Table 1. Good agreement between calculated and measured energies can be noticed. The excitation energies of the $4p^55s^25p$ levels, wavelengths, and probabilities for the $(4p^55s^25p)\,^{1,3}L_J \rightarrow (4p^54d5s^2)\,^3\mathrm{P}_{1,2}$, $^3\mathrm{F}_4$ radiative transitions are presented in Table 2.

Table 1. Excitation energies E_{exc} (in eV) with respect to the $(4p^65s^2)\,^1\mathrm{S}_0$ ground state and oscillator strength gf of strontium lowest atomic autoionising states calculated in single-configuration Hartree–Fock approximation and compared with experimental data E_{exp}. Symbols E1 and M2 mark electric dipole and magnetic quadrupole transitions.

Configuration	State	E_{exc}	gf	E_{exp}
$4p^54d5s^2$	$^3\mathrm{P}_0$	20.758	0.00	20.98
$4p^54d5s^2$	$^3\mathrm{P}_1$	21.049	2.132−03 (E1)	21.12
$4p^54d5s^2$	$^3\mathrm{P}_2$	21.347	1.282−09 (M2)	21.38
$4p^54d5s^2$	$^3\mathrm{F}_4$	21.545		21.62
$4p^55s4d^2$	$^3\mathrm{P}(^3\mathrm{F})^5\mathrm{D}_0$	21.374		
$4p^55s4d^2$	$^3\mathrm{P}(^3\mathrm{F})^5\mathrm{D}_1$	21.391		
$4p^55s4d^2$	$^3\mathrm{P}(^3\mathrm{F})^5\mathrm{D}_2$	21.425		
$4p^54d5s^2$	$^3\mathrm{F}_3$	21.789		21.82
$4p^54d5s^2$	$^3\mathrm{F}_2$	22.242	5.997−11 (M2)	22.06
$4p^55s4d^2$	$^3\mathrm{P}(^3\mathrm{P})^5\mathrm{P}_2$	22.443		

For the $4p^54d5s^2$ configuration a very strong mixing between the terms $^3\mathrm{D}_3$ and $^1\mathrm{F}_3$ as well as $^3\mathrm{D}_2$ and $^1\mathrm{D}_2$ was noticed, resulting in the ambiguity of the assignment of the total angular momenta LS. The same strong mixing also exists between $^3\mathrm{D}_2$ and $^1\mathrm{D}_2$ as well as $^3\mathrm{P}_0$ and $^1\mathrm{S}_0$ states in $4p^55s^25p$ configuration. In the case of $4p^55s4d^2$ configuration, the problem with the assignment of the LS terms does not exist as the leading term is obvious. For example, for the states listed in Table 1, the expansion coefficients are 0.73 for $^3\mathrm{P}(^3\mathrm{F})^5\mathrm{D}_0$, 0.90 for $^3\mathrm{P}(^3\mathrm{F})^5\mathrm{D}_1$, 0.87 for $^3\mathrm{P}(^3\mathrm{F})^5\mathrm{D}_2$, and 0.96 for $^3\mathrm{P}(^3\mathrm{P})^5\mathrm{P}_2$.

4. Results

The excitation functions for the most efficiently excited autoionising states at 21.12, 21.38, and 21.62 eV are shown in Fig. 2 in an impact energy range from the excitation threshold of states up to 200 eV. As can be seen, all functions possess nearly similar shape characterized by the presence of the narrow near-threshold maxima, features *E*, *F*, *G*, and the broad main maxima located at 32 eV ($^3\mathrm{P}_{1,2}$) and 35 eV ($^3\mathrm{F}_4$). The insets show the near-threshold parts of excitation functions where the 'fine' structure *a–d* is observed. The energy positions of these features are given in Table 3.

As it follows from the analysis of the intensity behaviour of lines in ejected electron spectra measured at low impact energies (see also [5, 8]), those of lines located in electron spectra at 15.29, 15.43, 15.69, and 15.93 eV are due to ejected electrons coming from the autoionising levels with the lowest excitation

Table 2. Excitation energies $E_{\rm exc}$ (in eV) with respect to the $(4p^6 5s^2)\,{}^1\mathrm{S}_0$ ground state for the levels $(4p^5 5s^2 5p)\,{}^{1,3}L_J$ calculated in single-configuration Hartree–Fock approximation, probabilities A (in s^{-1}), and wavelengths λ (in nm) for the radiative transitions $(4p^5 5s^2 5p)\,{}^{1,3}L_J \to (4p^5 4d 5s^2)\,{}^3\mathrm{P}_{1,2}$, ${}^3\mathrm{F}_4$ levels in strontium.

$(4p^5 5s^2 5p)\,{}^{1,3}L_J$	$E_{\rm exc}$	$(4p^5 4d\,5s^2)\,{}^3L_J$	A	λ
${}^3\mathrm{S}_1$	22.98	${}^3\mathrm{P}_1$	1.87+05	363
		${}^3\mathrm{P}_2$	7.27+06	760
${}^3\mathrm{D}_3$	23.27	${}^3\mathrm{F}_4$	1.29+07	782
${}^3\mathrm{D}_2$	23.28	${}^3\mathrm{P}_2$	1.86+05	642
		${}^3\mathrm{P}_1$	7.92+05	556
${}^1\mathrm{P}_1$	23.46	${}^3\mathrm{P}_2$	1.96+06	588
		${}^3\mathrm{P}_1$	4.55+05	515
${}^3\mathrm{P}_2$	23.51	${}^3\mathrm{P}_2$	8.27+06	573
		${}^3\mathrm{P}_1$	3.62+06	504
${}^3\mathrm{P}_0$	23.85	${}^3\mathrm{P}_1$	9.49+06	442
${}^3\mathrm{D}_1$	24.34	${}^3\mathrm{P}_2$	1.65+05	415
		${}^3\mathrm{P}_1$	1.39+06	377
${}^1\mathrm{D}_2$	24.44	${}^3\mathrm{P}_2$	4.68+06	401
		${}^3\mathrm{P}_1$	5.30+05	365
${}^3\mathrm{P}_1$	24.46	${}^3\mathrm{P}_2$	1.53+07	398
		${}^3\mathrm{P}_1$	1.87+05	363
${}^1\mathrm{S}_0$	24.82	${}^3\mathrm{P}_1$	1.12+07	328

Table 3. Energy positions (in eV) and tentative classification of features observed in ejected electron excitation functions of the $(4p^5 4d 5s^2)\,{}^3L_J$ autoionising states in strontium atoms. Signs $+/-$ mark presence / absence of features in excitation function of corresponding state.

Feature	Position	${}^3\mathrm{P}_1$	${}^3\mathrm{P}_2$	${}^3\mathrm{F}_4$	Classification
a	21.6	+	+	−	$4p^5 5s^2 4d^2$
b	22.1	−	+	+	−"−
c	22.5	+	−	−	−"−
d	22.8	−	+	−	−"−
E	24.3	+	−	−	$(4p^5 5s^2 5p)\,{}^3L \to (4p^5 4d 5s^2)\,{}^3\mathrm{P}_1 + h\nu$
F	25.5	−	+	−	$(4p^5 5s^2 5p)\,{}^3L \to (4p^5 4d 5s^2)\,{}^3\mathrm{P}_2 + h\nu$
G	24.8	−	−	+	$(4p^5 5s^2 5p)\,{}^3L \to (4p^5 4d 5s^2)\,{}^3\mathrm{F}_4 + h\nu$

thresholds at 20.98, 21.12, 21.38, and 21.62 eV, respectively. A similar shape of the excitation functions for these states (see Fig. 2) reflects the common exchange character of electron transitions from the $(4p^6 5s^2)\,{}^1\mathrm{S}_0$ ground state of Sr atom and, consequently, the triplet character of the corresponding excited states. As it follows from the comparison of our single-configuration Hartree–Fock calculations and experimental data [4] (see Table 1), there is an excellent agreement between both sets of data for the $(4p^5 4d 5s^2)\,{}^3\mathrm{P}_{0,1,2}$ and ${}^3\mathrm{F}_4$ autoionising states. Although the location of the ${}^3\mathrm{P}({}^3\mathrm{F}){}^5\mathrm{D}_{0,1,2}$ states from $4p^5 5s 4d^2$ configuration is also predicted close to the same experimental energies, however, due to the two-electron character of excitation of these states, their excitation cross-section should be smaller than that for the ${}^3\mathrm{P}$ and ${}^3\mathrm{F}$ states from the $4p^5 4d 5s^2$ single-electron configuration. Therefore, one may conclude that $(4p^5 4d 5s^2)\,{}^3\mathrm{P}_{0,1,2}$ and ${}^3\mathrm{F}_4$ states are the lowest $4p^6$-core excited atomic autoionising states in strontium atoms. On the same grounds the lines with excitation thresholds at 21.82 and 22.06 eV were attributed to the decay of the $(4p^5 4d 5s^2)\,{}^3\mathrm{F}_{3,2}$ high-lying autoionising states. Figure 3 shows the energy level diagram of strontium atoms in the region of the $4p^5 4d 5s^2$ classified levels and the relative position of features observed in the measured excitation functions.

5. Discussion

To analyse the excitation dynamics of the $(4p^5 4d 5s^2)\,{}^3\mathrm{P}_{1,2}$ and ${}^3\mathrm{F}_4$ autoionising states, let us consider the

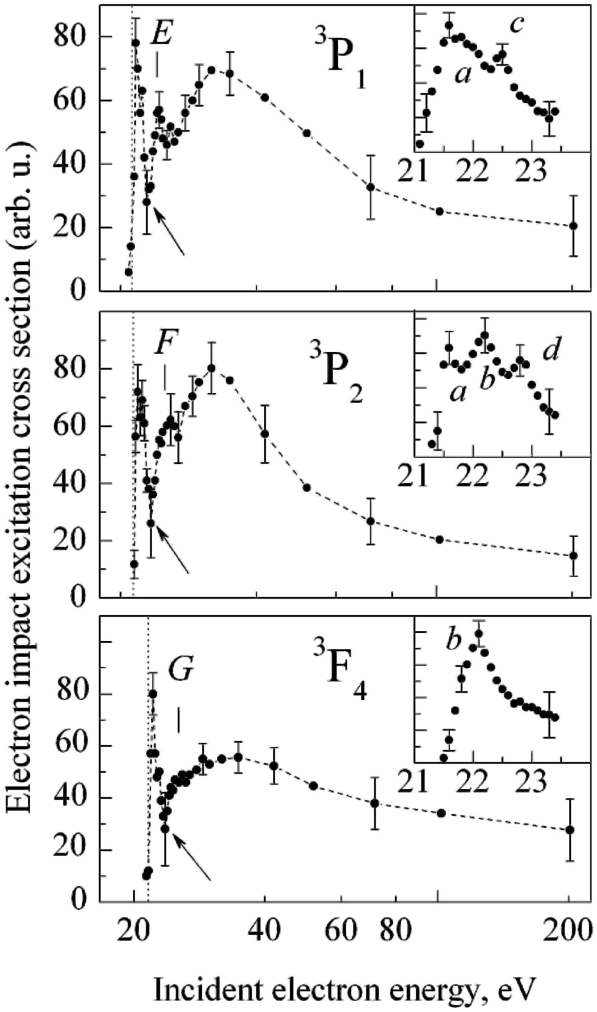

Fig. 2. The ejected electron excitation functions for the $(4p^5 4d5s^2)\,^3\mathrm{P}_1$, $^3\mathrm{P}_2$, and $^3\mathrm{F}_4$ autoionising states in strontium. Dot lines mark the excitation thresholds at 21.12, 21.38, and 21.62 eV, respectively. Arrows mark the appearance thresholds for the features *E*, *F*, *G* (see text). Insets show the near-threshold parts of excitation functions.

processes which may contribute to their electron impact excitation, i. e.

$$\mathrm{Sr}(4p^6 5s^2)\ {}^1\mathrm{S} + \mathrm{e}_{\mathrm{inc}} \rightarrow$$

$$\begin{cases} \mathrm{Sr}^*(4p^5 4d5s^2)\,{}^3L + \mathrm{e}_{\mathrm{sc}}\,, & (1) \\ \mathrm{Sr}^*(4p^5 n_1 l_1 n_2 l_2 n_3 l_3)\,{}^3L + \mathrm{e}_{\mathrm{sc}} & (2) \\ \quad\downarrow \\ \mathrm{Sr}^*(4p^5 4d5s^2)\,{}^3L + h\nu\,, \\ \mathrm{Sr}^-(4p^5 n_1 l_1 n_2 l_2 n_3 l_3)\,\varepsilon l & (3) \\ \quad\downarrow \\ \mathrm{Sr}^*(4p^5 4d5s^2)\,{}^3L + \mathrm{e}_{\mathrm{ej}}\,. \end{cases}$$

Reaction (1) represents the direct spin-exchange excitation of the $4p^6$ subshell in strontium. As it follows from the general considerations [19], this process has a resonance character and should play an important role at low and intermediate impact energies. Reaction (2) describes the cascade population of the $4p^5 4d5s^2$ states due to the radiative transitions from the high-lying autoionising states (see Fig. 3). Note that such transitions may posses a remarkable efficiency in strontium due to the presence of strong level mixing effects in $4p^6$ excitation [9, 10]. Finally, reaction (3) represents the resonance excitation of the $(4p^5 4d5s^2)\,^3L$ states through the creation and subsequent electron decay of short-lived states of the Sr^- ion. The presence of strong near-threshold resonances in all the measured excitation functions undoubtedly points out an important role of reaction (3) at low impact energies. Below, by using all available experimental and theoretical data on excitation of the $4p^6$ subshell in strontium, we will attempt to evaluate the contribution of each process to electron impact excitation of the $4p^5 4d5s^2$ states.

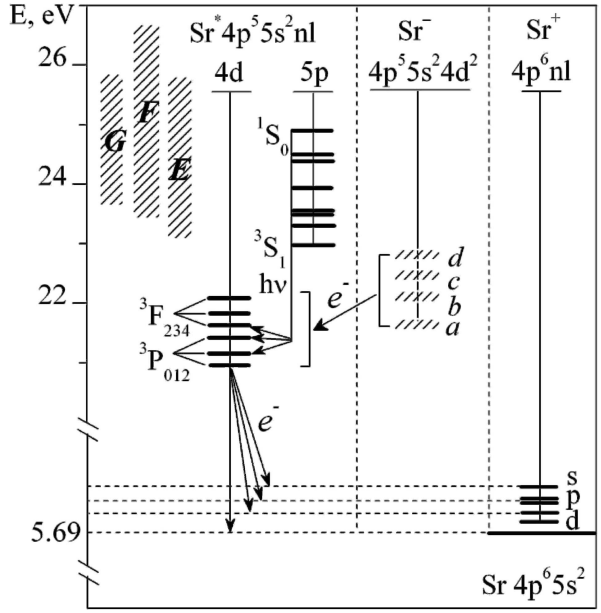

Fig. 3. The energy level diagram for strontium atom. Only the levels participating in processes (1)–(3) are shown.

Direct electron impact excitation. The single-electron character of the transition and the lowest excitation thresholds both provide high direct excitation efficiency for the $4p^5 4d5s^2$ configuration. Indeed, most of the strong lines observed in ejected electron [4–6] and in photoabsorption spectra [9] represent the excitation just of this configuration. As it follows from the present data (see Fig. 3), a relatively low energy of the main excitation maxima and a fast decrease of the cross-section above 40 eV both confirm the spin-exchange character of direct excitation of the $^3\mathrm{P}_{1,2}$ states. A broadened shape of the main maximum and a

slower decrease of the cross-section observed for the $^3F_4$ state may indicate an influence of singlet states from $4p^5 5s 4d^2$ and $4p^5 5s^2 6s$ neighbouring configurations due to the configuration mixing effect [10].

Cascade processes. The thresholds for the features *E*, *F*, *G* to appear are 23.1, 23.4, and 23.6 eV, respectively (see arrows in Fig. 2). These values differ from the energy positions of corresponding maxima by 1–2 eV. As the energy resolution of the present measurements has been <0.2 eV, one may conclude that the features *E*, *F*, *G* possess a compound character and their origin represents some superposition of processes (2) and (3). The cascade population of the $(4p^5 4d 5s^2)\,^3L$ levels in strontium (process (2)) can be caused by the radiative transitions from the high-lying even configurations. As it follows from the present calculations (see Table 2), such nearest configuration is $4p^5 5s^2 5p$. Comparison of the position of this configuration relative to features *E*, *F*, *G* (see energy level diagram in Fig. 3) shows that the apparent thresholds of features fit well the location of the $^3S_1$, $^3D_2$, $^3P_2$, $^1P_1$, and $^3P_0$ lowest levels, whereas their maxima are located in the region of the $^3D_1$, $^3P_1$, and $^3S_0$ upper levels. All the above states possess two decay modes: non-radiative (autoionisation) and radiative. The first one results in ejected electron lines at energies between 17.5 and 20.0 eV. As it follows from the analysis of ejected electron spectra measured at low impact energies [5, 8], these lines possess relatively low intensities, reflecting by that the low autoionisation probabilities for the corresponding levels. Second decay mode has, in turn, two competitive channels: into the $4p^5 4d 5s^2$ nearest autoionising levels and into the $4p^6 n_1 l_1 n_2 l_2$ atomic states. As to the latter process, former data by Aleksakhin et al. [7] revealed only two weak lines at 58.4 and 62.4 nm, which were classified as an assumed radiative decay of an unidentified state at 23.45 eV into the $(4p^6 5s 4d)\,^3D_3$ and $(4p^6 5s 6s)\,^3S_1$ atomic states, respectively. From the present calculations it follows that among all radiative transitions $4p^5 5s^2 5p \rightarrow 4p^5 4d 5s^2$ those into the $(4p^5 4d 5s^2)\,^3P_{1,2}$, $^3F_4$ levels are the most probable ones (see Table 2). Therefore, one may conclude that features *E*, *F*, *G* reflect indeed a summed radiative cascade contribution from the $4p^5 5s^2 5p$ levels. Moreover, an abrupt rise of the cross-section above the thresholds of features *E*, *F*, *G* and an evident resonance shape of features *E* and *F* all point out an important role of negative-ion resonances (reaction (3)) in excitation of the cascading levels. Note that such 'resonance' cascades were earlier observed in electron impact excitation of low-lying autoionising states in lithium [14] and potassium [17] atoms.

Resonance excitation. Within the bounds of Schulz's classification scheme for negative-ion resonances [20], features *a–d* may reflect the electron decay either of shape- or Feshbach-type resonances built on the $4p^5 4d 5s^2$and $4p^5 5s 4d^2$ 'parent' autoionising configurations (see Table 1). As mentioned above, neither theoretical nor experimental data are known on $4p^6$-core excited negative-ion resonances in strontium atoms. In order to establish, at least tentatively, the spectroscopic classification of observed structure, we have applied the known method of comparison of *isoelectronic* configurations [6]. If the $4p^5 4d 5s^2$ configuration is considered as a 'parent' one for the $(4p^5 4d 5s^2)\,\varepsilon l$ states of Sr^{*-} ion ($Z = 38$) (see reaction (3)), then the nearest *isoelectronic* configurations could be the $4p^5 4d 5s^2 nl$-core excited configurations of neutral yttrium ($Z = 39$) [21]. In accordance with the calculations [22], the $4p^5 5s^2 4d^2$ configuration is the lowest in yttrium atom and possesses the highest excitation efficiency. Therefore, one may suppose that the same configuration will be the lowest one also in strontium negative ion. In this case, fast electron decay of states from this configuration will result in appearance of the structure *a–d* in excitation functions of the $(4p^5 4d 5s^2)\,^3P_{1,2}$ and $^3F_4$ states (see Figs. 2, 3). The presence of features *a*, *b* simultaneously in excitation functions of the $^3P_1$ and $^3P_2$ levels shows that the corresponding negative ion states possess two-channel decay mode. Finally, comparing the excitation efficiency of processes (1) and (3) (see Fig. 2) it is seen that the resonance excitation cross-section for the $^3P_{1,2}$ states is approximately equal to that for the direct excitation, but it is higher by approximately $1/3$ in the case of the $^3F_4$ state.

6. Conclusions

This work is the first study of excitation dynamics of the $4p^6$-core excited autoionising states in strontium atoms performed with high energy resolution over a wide electron impact energy range from the lowest excitation threshold up to 200 eV. By using the results of single-configuration Hartree–Fock calculations, the spectroscopic classification of six lowest autoionising states was established. The performed analysis of ejected electron excitation functions for the $(4p^5 4d 5s^2)\,^3P_{1,2}$, $^3F_4$ states has showed that along with spin-exchange direct excitation, two other processes determine the electron impact excitation of these states, namely, the electron decay of the $4p^5 5s^2 4d^2$ states of

strontium negative ion, and the radiative cascade transitions from the $4p^5 5s^2 5p$ autoionising states. For the $^3P_{1,2}$ states the resonance excitation cross-section is approximately equal to that for the direct excitation, but it is higher by approximately $1/3$ in the case of the $^3F_4$ state. The cascade contribution is considerable for all states studied. Its resonance character reveals an important role of negative ions also in the excitation of the $4p^5 5s^2 5p$ cascading levels.

Acknowledgements

We wish to acknowledge the financial support from INTAS under grant No. 03-51-4706 (A. B.) and from Taiwan–Baltic project (A. K.).

References

[1] S. Okudajra, J. Phys. Soc. Jpn. **29**, 409 (1970).
[2] B. Peart and K. Dolder, J. Phys. B **8**, 56 (1975).
[3] S.T. Chen, D. Leep, and A. Gallagher, Phys. Rev. **13**, 977 (1976).
[4] M.D. White, D. Rassi, and K.J. Ross, J. Phys. B **12**, 315 (1979).
[5] A.A. Borovik, I.S. Aleksakhin, A.V. Kupliauskiene, and V.F. Bratsev, Opt. Spectrosk. [Opt. Spectrosc. (USSR)] **53**, 976 (1982).
[6] S.J. Buckman and C.W. Clark, Rev. Mod. Phys. **66**, 539 (1994).
[7] I.S. Aleksakhin, G.G. Bogachev, I.P. Zapesochny, and S.Yu. Ugrin, Zh. Eksp. Teor. Fiz. **80**, 2187 (1981) [Sov. Phys. JETP **53**, 1140 (1981)].
[8] S.M. Kazakov and O.V. Khristoforov, Zh. Eksp. Teor. Fiz. [Sov. Phys. JETP] **88**, 1118 (1985).
[9] M.W.D. Mansfield and G.H. Newsom, Proc. R. Soc. London A **377**, 431 (1981).
[10] J.P. Connerade, M.A. Baig, and M. Sweeney, J. Phys. B **23**, 713 (1990).
[11] P. Marmet and L. Kerwin, Can. J. Phys. **38**, 787 (1960).
[12] A.A. Borovik, Prib. Tekh. Eksp. [Instrum. Exp. Tech. (USSR)] **34**, 124 (1991).
[13] A.A. Borovik, H. Rojas, and G.C. King, Meas. Sci. Technol. **6**, 334 (1995).
[14] A.A. Borovik and V.N. Krasilinec, J. Phys. B **32**, 1941 (1999).
[15] O.O. Borovik, Ukr. J. Phys. **45**, 1270 (2000).
[16] A. Kupliauskienė, P. Bogdanovich, and A. Borovik, Lithuanian J. Phys. **47**, 7 (2007).
[17] A. Kupliauskienė, P. Bogdanovich, A.A. Borovik, O. Zatsarinny, and K. Bartschat, J. Phys. B **39**, 591 (2006).
[18] Ch. Froese Fischer, Comput. Phys. Commun. **43**, 355 (1987).
[19] H.S.W. Massey and H.B. Gilbody, *Electronic and Ionic Impact Phenomena*, 2nd ed. (London, Oxford University Press, 1974).
[20] G.J. Schulz, Rev. Mod. Phys. **45**, 378 (1973).
[21] W.C. Martin, J.R. Fuhr, D.E. Kelleher, A. Musgrove, J. Sugar, W.L. Wiese, P.J. Mohr, and K. Olsen, *NIST Atomic Spectra Database (Version 2.0)* (National Institute of Standards and Technology, Gaithersburg, MD, 1999), `http://physics.nist.gov/asd`.
[22] W. Wijesundera and H.P. Kelly, Phys. Rev. A **36**, 3187 (1987).

AUTOJONIZACINĖS STRONCIO ATOMO BŪSENOS SU VAKANSIJA 4p ELEKTRONŲ SLUOKSNYJE: JŲ KLASIFIKAVIMAS IR SUŽADINIMO DINAMIKA

A. Borovik [a], V. Vakula [a], A. Kupliauskienė [b]

[a] *Ukrainos NMA Elektronų fizikos institutas, Užgorodas, Ukraina*
[b] *VU Teorinės fizikos ir astronomijos institutas, Vilnius, Lietuva*

Santrauka

Išmatuotas iš stroncio atomų išlėkusių elektronų spektras, atitinkantis šuolius iš žemiausių $4p^5 n_1 l_1 n_2 l_2 n_3 l_3$ būsenų, kai žadinančio elektrono energija buvo keičiama nuo sužadinimo slenksčio iki 200 eV. Panaudojant vienkonfigūracinio Hatrio ir Foko artinio skaičiavimo duomenis, identifikuotosios šešios išlėkusių elektronų linijos, kurių energijos yra arčiausiai sužadinimo slenksčio, priskirtos $4p^5 4d5s^2\ ^3P_{0,1,2}$ ir $^3F_{2,3,4}$ autojonizacinėms būsenoms. $4p^5 4d5s^2\ ^3P_{1,2}$ ir $^3F_4$ būsenų sužadinimo funkcijos išmatuotos, keičiant žadinančio elektrono energiją kas 0,15 eV. Visose šiose sužadinimo funkcijose prie sužadinimo slenksčio pirmą kartą pastebėti didelio intensyvumo rezonansai. Jų atsiradimas aiškinamas stroncio atomo neigiamo jono $4p^5 5s^2 5p^2$ konfigūracijos trumpaamžių būsenų autojonizacija. Panaudojant apskaičiuotas Hartrio ir Foko artinyje radiacinių šuolių iš $4p^5 5s^2 5p$ konfigūracijos lygmenų tikimybes ir energijas, įvertintas kaskadų iš $4p^5 5s^2 5p$ konfigūracijos būsenų indėlis, apgyvendinant $4p^5 4d5s^2\ ^3P_{0,1,2}$ ir $^3F_{2,3,4}$ lygmenis.